

# Observation of two-dimensional melting of vortex lattices in a superconducting transformer

S. I. Moskvina

*Institute of Solid State Physics, USSR Academy of Sciences*

(Submitted 30 November 1984)

*Zh. Eksp. Teor. Fiz.* **88**, 2148–2157 (June 1985)

A Kosterlitz-Thouless solid-liquid transition was observed by the superconducting-transformer method in a system of two-dimensional vortices. Dragging of the magnetic structure in granulated Al films separated by a dielectric carbon layer was investigated. The modification of the solutions of the diffusion equations for the vortex motion by allowance for pinning are considered. The phase transition, meaning the melting of the vortex lattice, was detected by the change of the transformer response when the temperature was raised. The vortex-lattice melting temperatures were measured in superconducting films of various thicknesses. The experimental relations reveal the predicted singularities associated with the action of the pinning centers. The feasibility of studying the details of the melting process by the indicated method is demonstrated.

To explain and predict the behavior of mixed-state superconductors in a number of cases it is important that the model (of the vortex liquid or the vortex crystal) conform to the real situation in the sample. This pertains, e.g., to problems connected with the nonlinearity of the current-voltage characteristics (IVC), with the peak effect near the upper critical field  $H_{c2}$ , and with fluctuations of the conductivity near the critical temperature  $T_c$ . At the same time, the obvious or easily calculated changes that occur in superconductor characteristics, most frequently in the IVC, when a vortex crystal liquefies are experimentally so small<sup>1</sup> that they cannot reliably attest to such a transition. Methods of directly observing the magnetic structure<sup>2</sup> do not permit, by virtue of procedural features, to determine exactly the experimental conditions,<sup>1</sup> namely the temperature and the magnetic field, and furthermore yield information only on the stationary state of the magnetic structure and can only approximately describe it in the course of motion, in the resistive region.

Melting of vortex lattices (gradual vanishing of long-range order in them) can be caused either by temperature fluctuations<sup>1</sup> or by "disordering" of the lattices by pinning centers.<sup>3</sup> The two processes, which are probably additive, break up the lattice into blocks, and in the limit of the vortex liquid the block dimensions become of the order of the lattice parameter.

In thin superconducting mixed-state films there can be no long-range order in the traditional coordinate representation, since this order is destroyed at finite temperatures by the long-wave phonons. At the same time, depending on the response of the system to weak external action, one can speak of the existence of a topological long-wave order that is preserved under continuous and mutually unique mappings of the system. At low temperatures the vortex lattice should preserve an elastic response to an external action also in two dimensional systems. With rising temperature, owing to the formation of free dislocation in the system, its response to an external perturbation becomes viscous and liquid-like.<sup>4</sup> No such phase transitions were previously ob-

served in a system of superconducting vortices.<sup>2)</sup> The two-dimensionality criterion for a vortex crystal with an order of the Kosterlitz-Thouless type is connected with the possibility of neglecting the fluxural elastic moduli  $C_{44}$ . This is possible either in the case of thin films of thickness  $d < \lambda_1$  (magnetic-field penetration depth), or in cases of  $C_{44}$  very large compared with the thermal perturbation. The latter can apparently be realized in superconductors with the limiting values of the parameter  $\kappa$ , at which the sign of the vortex interaction is reversed.<sup>7</sup>

Superconducting films separated by a dielectric layer thin enough to permit magnetic coupling between the vortex sublattices in the films (Giaever transformer) can be used as the instrument for observing the melting of the lattices in these films.

We report here an experimental investigation of the characteristics of a Giaever transformer in the lattice-melting regime and an observation of a topological phase transition in a two-dimensional system of superconducting vortices. The first part contains a basic analysis of the transformer operation in the lattice-melting regime and with the changes produced in the lattices when account is taken of the uniformly distributed pinning centers. The experimental procedure is described in the second part. The third part contains the measured IVC of the transformer and a comparison with the model. During the present stage of the work, a film with sufficiently high pinning force was used. Pinning inhomogeneities of the films should have lowered the phase-transition temperature, and this facilitated the experimental observation of this phenomenon.

## 1. CONDITIONS FOR VORTEX DRAG IN A GIAEVER TRANSFORMER

The very possibility of a considerable drag of vortices in a superconducting transformer is due to the existence of their ordered arrangement and to the presence of interaction between them. In a model in which the vortices are isolated and constitute a vortex liquid without short-range order, it is found that the potential relief produced by the vortices in the

primary film is substantially smaller (by one or two orders) than the size of the thermal fluctuations.<sup>8</sup> Simple estimates show that the Brownian behavior of the vortices suppresses the drag in this case. If the vortices are bound, the potential relief becomes proportional to their number and can substantially exceed the thermal fluctuations. Vortex drag can occur also in films in which the pinning force is weaker than the magnetic interaction between the films. Otherwise, when the magnetic structure is moved over the primary film by the transport current, it cannot cause motion of the vortices in the secondary force. The vortex mutual drag force is connected with the film thickness  $d$ , with the insulator-layer thickness, and with the distance between them. The maximum value of this force (per vortex), in the approximation where the potential relief is sinusoidal, is given by<sup>9</sup>

$$f_0 \approx \tilde{f} 3 \Phi_0 d_1 d_2 / 32 \pi^3 \lambda_L^4; \quad (1)$$

here  $\Phi_0$  is the flux quantum and  $\lambda_L$  is the London magnetic-field penetration depth. The coefficient  $\tilde{f}$  is connected only with the insulator thickness and with the distance between the vortices. Motion of the vortices in the secondary film is hindered by the pinning forces  $f_p$  and by the viscous forces  $f_v$ . When velocities are reached such that  $f_0 \leq f_p + f_v$ , relative slippage of the lattices beings, and a square-root singularity should be observed on the IVC of the transformer.<sup>10</sup> When the vortex lattices melt as a result of a weakening of the drag, the transformer IVC are qualitatively changed. Compared with the voltage  $V_1$  on the primary film, the voltage  $V_2$  on the secondary decreases and the square-root singularity of the IVC vanishes.

The authors of Ref. 8 calculated the characteristics of the superconducting transformer in the case of lattice melting, without allowance for the pinning forces. The calculations were based on a solution of the diffusion equations for the vortices in the potential relief produced by the moving vortex system in the primary film. The diffusion coefficient  $D$  was assumed equal to  $T/\eta$ , where  $\eta$  is the vortex viscosity in the film

$$\eta \approx \Phi_0 H_{c2}(T) d / \rho_n c^2; \quad (2)$$

where  $\rho_n$  is the resistivity of the film in the normal state and  $c$  is the speed of light. Solution of the diffusion equation for the vortex distribution function in the primary and secondary films jointly with the electrodynamics equations of the magnetic structure leads to an expression that relates the voltage  $V_1$  in the primary film (the only film that carries the transport current  $I$  causing the dynamic state of the entire transformer) and the voltage  $V_2$  in the secondary film

$$V_2 = \frac{1}{16\pi} \frac{L \Phi_0 H^2 T}{\lambda_{\perp}^3 \eta^2 c^2 V_1} \ln \left\{ 1 + \frac{\pi}{4} \frac{\lambda_{\perp} c \eta^2 V_1}{T L^2 H^3 \Phi_0} \right\}; \quad (3)$$

here  $L$  is the linear dimension of the transformer.

Equation (3) is valid for temperatures  $T \gg T_M$ , where  $T_M$  is the solid-liquid phase-transition temperature and is given by<sup>1</sup>

$$T_M = \Phi_0^2 A / 64 \sqrt{3} \pi^3 \lambda_{\perp}(T_M), \quad (4)$$

if the magnetic field satisfies the condition

$$\xi^{-2}(T) \gg H / \Phi_0 \gg \lambda_{\perp}^{-2}(T).$$

Here  $\xi(T)$  is the coherence length and  $A = 0.4$  to  $0.75$  is a combination of the lattice elastic moduli.

The maximum value of the secondary voltage is reached at

$$V_1 = \left( \frac{4 \Phi_0^2}{\pi \lambda_{\perp} T} \right)^{1/2} \frac{L H^3 T}{\eta c \Phi_0^{1/2}}; \quad (5)$$

this leads to

$$V_{2 \max} = \frac{1}{80} \frac{\Phi_0}{H \lambda_{\perp}^2} V_1. \quad (6)$$

In this case the magnetic field must satisfy the very lax condition

$$\Phi_0 \eta \lambda_{\perp} / 4 \pi T \gg 1.$$

It can be seen that this analysis does not take into account the vortex pinning that is always present, to a greater or lesser degree, in real samples. As indicated in Ref. 1, allowance for the pinning forces shifts the melting temperature by an amount  $T$ , so that

$$\Delta T / T_M \sim b^2 / a_0^2. \quad (7)$$

Here  $b$  is the distance between the uniformly distributed weak pinning centers and  $a_0$  is the vortex-lattice parameter.

By virtue of the linear relation, implied in the model of Ref. 8, between the voltage  $V$ , the transport current  $I$ , and the vortex velocity  $v$ , introduction of extraneous pinning forces into the solution of the diffusion differential equation will not change the foregoing analysis of the transformer operation, and the final result (3) will retain the same form. The statement, however, that the diffusion coefficient is equal to  $T/\eta$  is no longer valid, since the motion of the secondary lattice is hindered by the viscous forces on top of the pinning forces. We can introduce a certain effective viscosity

$$\eta_{\text{eff}} = \eta + f_p / v_2, \quad v_2 = V_2 c / L H, \quad (8)$$

that takes into account the delay of the vortex motion by the pinning. Equation (3) is then transformed in first-order approximation, without allowance for the change in the term under the logarithm sign, as follows:

$$V_{2p} = V_2 - f_p L H / c \eta. \quad (9)$$

Here  $V_2$  is the same as in Eq. (3).

It can be seen from (9) that in the linear IVC model the specific allowance for the pinning forces should alter not only the temperature and field dependences of the transformer IVC, but the IVC themselves. Specifically, immediately after the secondary lattice is set a difference  $f_p L H / c \eta$  should set in between  $V_1$  and  $V_2$ , and should manifest itself on the transformer IVC plotted in the real experimental scale as a difference between the critical cutoff currents in the primary and secondary lattices. One more manifest feature of allowance for pinning is a nonmonotonic dependence, which follows from expressions (6) and (9), of the maximum secondary voltage on the magnetic field.

## 2. SAMPLES AND MEASUREMENT PROCEDURE

The measured transformers were granulated Al films of uniform thickness, sputtered on quartz substrates at room temperature. The sputtering was from a tungsten-wire electrode, at a rate  $10 \text{ \AA/s}$  and at an oxygen pressure  $1.5 \cdot 10^{-5}$  Torr in the chamber. The distance from the sample to the evaporator was 10 cm. A general view of the transformer is shown in Fig. 1. The superconducting films were 0.1 cm wide. Each film had two pairs of contacts—potential and current. The distance between the potential contacts was 5 mm. After sputtering the first Al film the samples were kept for about 20 min at atmospheric pressure, after which an insulating carbon layer  $100 \text{ \AA}$  thick was sputtered on them in a vacuum  $10^{-6}$  Torr. The sputtered carbon came from two contacting small-area graphite electrodes located 4 cm from the substrate. The time to sputter the insulating film was 15 s. The second Al film was deposited on top of the insulating film. The resistance of the insulating film in the sandwich produced in this manner exceeded  $10^6 \Omega$ . The contacts were attached using conducting glue and secured to the substrate with epoxy adhesive. The directions of the external magnetic field  $H$ , of the transport current  $I$  in the primary field, of the electric field  $E$  in the secondary film, of the force  $f_L$  exerted by the transport current on the vortices in the primary film, and of the motion  $v$  of the vortices are all shown in Fig. 1.

We measured the IVC (the dependences of the voltages on the primary and secondary films on the transport current in the primary film) while varying the temperature and the external magnetic field. The measurements were performed in a cryostat with  $^4\text{He}$  vapor pumped off. The temperature of the liquid near the sample was measured with a semiconductor thermometer vapor-pressure-calibrated with a compression mercury manometer. The critical temperature  $T_c$  of the films was determined by a resistive method with  $50 \mu\text{A}$  flowing through the film.  $T_c$  was taken to be the temperature at which a voltage  $10^{-7} \text{ V}$  set in (start of the resistive transition). A typical resistive curve is shown in Fig. 2. The resistivity of the Al films was approximately  $5 \cdot 10^{-6} \Omega \cdot \text{cm}$ , and the variation from sample to sample was within several doz-

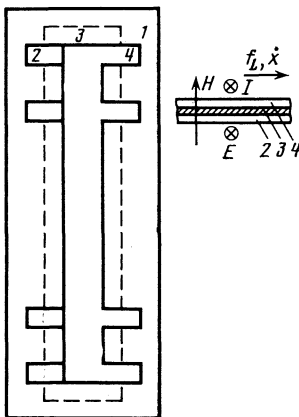


FIG. 1. General view of the employed superconducting transformers (the cross-section view shows the directions of the principal vectors). 1—Substrate, 2—secondary film, 3—insulator layer, 4—primary film.

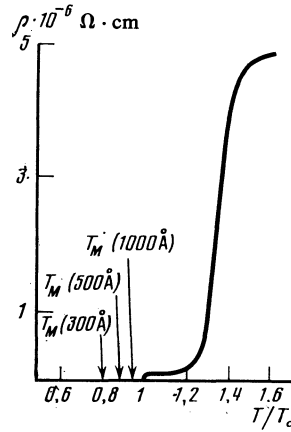


FIG. 2. Typical plot of resistive transition of a granulated film. The temperatures  $T_M$  of the topological phase transition are shown in the same scale for films 300, 500, and  $1000 \text{ \AA}$  thick.

en percent. We shall present data for three transformers with superconducting electrodes 300, 500, and  $1000 \text{ \AA}$  thick, chosen to have approximately equal pinning. The results for other transformers are approximately the same and support the tendency described below.

## 3. IVC OF TRANSFORMERS. TWO-DIMENSIONAL PHASE TRANSITION IN A SYSTEM OF SUPERCONDUCTING VORTICES

Figure 3 shows the IVC of a superconducting transformer. The curves are numbered in order of rising experimental temperature. These curves were plotted for all transformers in various magnetic fields and were the primary experimental data. The external magnetic field and the tem-

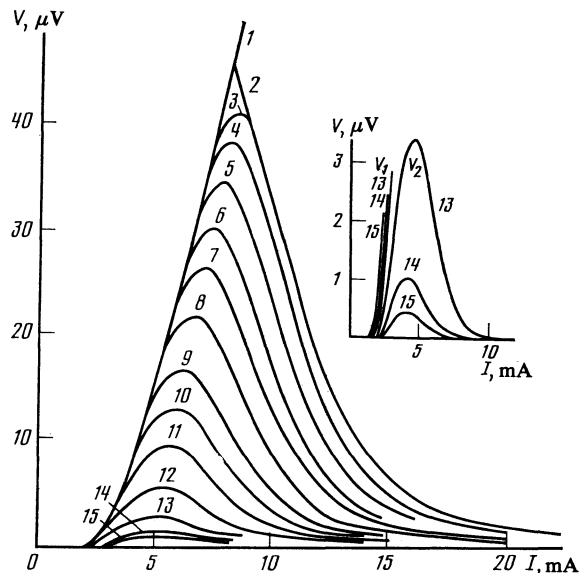


FIG. 3. IVC of transformer with superconducting electrodes  $500 \text{ \AA}$  thick. The inset shows the lower curves in enlarged scale: 1—primary IVC; 2—reconstructed secondary IVC of an ideal transformer; 3— $T = 1.252 \text{ K}$ , 4— $1.2536 \text{ K}$ , 5— $1.2552 \text{ K}$ , 6— $1.2568 \text{ K}$ , 7— $1.2584 \text{ K}$ , 8— $1.260 \text{ K}$ , 9— $1.2616 \text{ K}$ , 10— $1.2632 \text{ K}$ , 11— $1.2648 \text{ K}$ , 12— $1.2664 \text{ K}$ , 13— $1.2680 \text{ K}$ , 14— $1.270 \text{ K}$ , 15— $1.271 \text{ K}$ .

perature range corresponding to the IVC of Fig. 3 were purposefully chosen to make the variation of the primary IVC (curve 1) small enough to make them indistinguishable in the experimental scale employed. The appreciable change of the secondary IVC, i.e., the response of the transformer to the motion of the primary lattice, is clearly seen at the same time. The experiment demonstrates thus that the secondary IVC of a superconducting transformer is much more sensitive to the temperature changes of the film's superconducting properties than other characteristics, such as the critical current or the shape of the usual IVC.

At low temperatures (curve 3 of Fig. 3) the measured IVC are close to those of an ideal transformer.<sup>9</sup> On the predominant part of its height the secondary IVC duplicates the primary, but no square-root singularity is observed (cf. the reconstructed IVC of an ideal transformer—curve 2). The square-root singularity becomes successively smoother with rising temperature. At the highest temperatures (inset of Fig. 3) the IVC undergoes some qualitative changes. Even at the very lowest measured voltages the IVC's of the primary and secondary films have no common sections. A seeming difference between the critical points is observed and increases with decreasing temperature. Figure 4 shows the field dependence of the transformer IVC. It can be seen that the maximum secondary voltage has a nonmonotonic dependence on the magnetic field. Figures 3 and 4 show the experimental data for a transformer with superconducting electrodes 500 Å thick. The behavior of transformers with 300-, 500-, and 1000-Å superconducting electrodes is approximately the same. The drag effect proper decreased rapidly with decreasing film thickness, and at 300 Å it exceeded by merely an order of the resolving power ( $10^{-7}$ ) of the employed measuring system. The vortex-lattice melting temperature was determined from the instant of complete detachment of the secondary IVC of the transformer from that of the primary (curve 12 of Fig. 3). For comparison with the scale of the superconducting transition, the melting points of films of different thickness are shown in Fig. 2 together with the resistivity curve. It can be seen that  $T_M/T_c$  decreases with decreasing thickness of the superconducting electrodes of the transformer. Figure 5 shows the temperature dependence of the maximum secondary voltage  $V_M$ . At temperatures lower than  $T_M$  the plot vs.  $(1 - T/T_c)^2$  is nearly linear. At  $T \geq T_M$  this functional relation no longer holds.

If it is assumed that the smoothing of the square-root singularity on the IVC is evidence of relative slippage of the corresponding parts of the vortex lattices in the primary and secondary films, an enhancement of this process at higher temperatures attests to a decrease of the correlation dimension in the vortex structure. According to the premises developed in Ref. 4 concerning the topological long-range order, a phase transition of the solid-liquid type is determined primarily by the change of the system response to a small perturbation.

This response is elastic in the solid phase and viscous in the liquid. Vortex dragging allows us to apply this test to the investigated system of superconducting vortices. If the IVC of the primary and secondary films coincide, this means that despite the presence of viscous forces and pinning forces, the vortex-lattice velocity in the secondary film can follow that in the primary. As the vortex velocity increases (as  $V_1$  increases), the secondary IVC is separated from that of the primary (square-root singularity smoothing region). This means in fact that the elastic limit in the system has been exceeded and plastic flow sets in. With rising temperatures, as seen from Fig. 3, this detachment takes place at ever decreasing voltages  $V_1$ . Since a decrease of the critical value of  $V_1$  corresponds to a decrease of the critical velocity of the synchronous vortex motion in the films, and hence to a decrease in the limiting viscous force, one can speak of a decrease of the elastic limit of the investigated system as the temperature is raised. According to the definition above, this is in fact the temperature of the topological phase transition. With further rise of temperature the system behaves essentially in viscous manner even after the smallest perturbations (lowest velocities of the primary lattice). In the language of geometry this process corresponds to a lowering of the correlation size to  $a_0$ .

All the foregoing pertains only to the ascending branches of the IVC. On the descending sections the magnetic coupling force becomes smaller than the sum of the viscous and pinning forces, and our testing action simply does not reach entirely the vortex system in the secondary film.

Expression (4) allows us to calculate  $T_M$  and compare the experimental results with the theory, assuming that

$$\lambda_{\perp}(T_M) = \lambda_0^2 (\xi_0/2d) 1,33l(1 - T_M/T_c). \quad (10)$$

Here  $l$  is the mean free path. Substituting in (4) the material

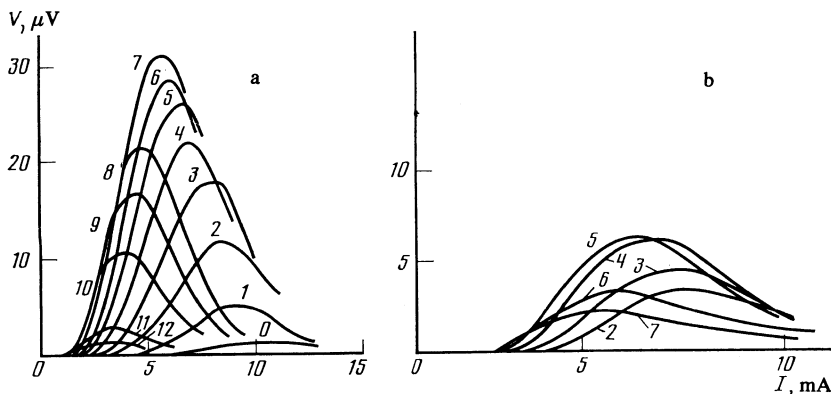


FIG. 4. Field dependence of the secondary IVC of a transformer with superconducting electrodes 500 Å thick; a)  $T = 1.26$  K—critical region; b)  $T = 1.268$  K—melting region of lattice  $H = (4 + n) \cdot 0.238$  Oe, where  $n$  is the number of the curve.

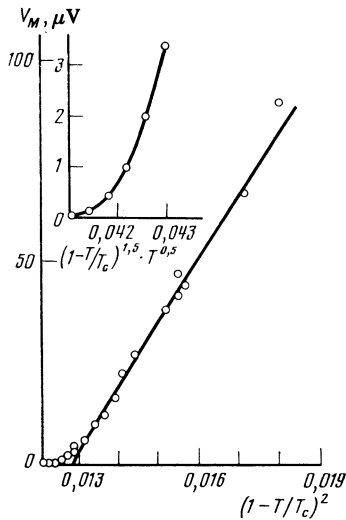


FIG. 5. Temperature dependence of maximum secondary voltage of transformer with superconducting-electrodes thickness 500 Å. Inset—start of curve in stretched scale. The abscissa scales correspond to the functional dependences on  $(1 - T/T_c)^2$  for the vortex-crystal regime and on  $(1 - T/T_c)^{1.5} \cdot T^{0.5}$  for the vortex liquid.

constants  $\lambda_0 = 5.15 \cdot 10^{-6}$  cm (Ref. 11),  $\xi_0 = 1.6 \cdot 10^{-4}$  cm,  $\rho_n l = 0.4 \cdot 10^{-11}$   $\Omega \cdot$  cm (Ref. 9),  $\rho_n = 5 \cdot 10^{-6}$   $\Omega \cdot$  cm, and  $A = 0.4$  we obtain the values of  $T_M^0$  listed in Table I together with the experimental values of  $T_c$  and  $T_M$ , the difference  $\Delta T$  between the calculated and experimental  $T_M$ , and the value of  $\Delta T/T_M^0$  for the investigated granulated Al films with different thicknesses  $d$ . We do not know unfortunately of any detailed calculations of the  $T_M$  shift due to the presence of the pinning force. This quantity can be estimated from (7). The values of  $a_0$  for the magnetic fields used in the experiment amount to several microns. At the same time, the granule size in the films with  $\rho_n = 5 \cdot 10^{-6}$   $\Omega \cdot$  cm is approximately 100 Å according to the data of Ref. 9. Comparison of these dimensions with the melting-temperature shift  $\Delta T/T_M^0$  shows that it is probably not the granule walls but some other large inhomogeneities which are the main pinning centers and influence the lowering of  $T_M$ . Assuming that these are inhomogeneities connected with the composition and sizes of the granules, the increase of  $\Delta T/T_M^0$  with decreasing film thickness becomes understandable. When the inhomogeneous films are sputtered, they simply become more isotropic with increasing thickness.

As already indicated, the presence of vortex pinning leads to certain qualitative changes of the transformer IVC. These peculiarities are clearly manifest on the experimental IVC. The inset of Fig. 3 shows clearly that at  $T > T_M$  the secondary IVC lag the primary ones. This does not mean,

however, that it is possible to separate the critical currents of the primary and secondary films of a system of magnetically coupled films. The reasoning that led to Eqs. (3) and (9) pertained to the dynamic state of the films and is valid only for the range of stable motion of the vortices. Under static conditions, however, the critical current of a superconducting transformer is, of course, perfectly single-valued. The decelerating action of the pinning centers is probably also the cause of the experimentally observed nonmonotonic dependences of the maximum secondary voltage on the strength of a weak magnetic field (Fig. 4). It can be seen from Figs. 4a and 4b that this peculiarity is a feature not only of a melted lattice ( $T = T_M$  in Fig. 4b), but also of the critical region prior to melting ( $T < T_M$  in Fig. 4b). The investigated phase transition can also be revealed by the temperature dependence of the maximum secondary voltage  $V_M$ . At  $T < T_M$  this dependence is close to linear (Fig. 5) when plotted against  $(1 - T/T_c)^2$ , in full agreement with the temperature dependence (1) of the maximum coupling force between the vortex lattices in a superconducting transformer. At  $T > T_M$  the  $V_M(T)$  dependence changes (inset of Fig. 5), and does not remain linear in terms of the coordinates  $(1 - T/T_c)^{1/5} T^{0.5}$ , as called for by the functional dependences of (5) and (6) on the temperature with account taken of (10).

The main temperature-induced changes of  $V_M$  occur in the region close to critical, while at higher temperatures the  $V_M(T)$  dependence becomes weaker (inset of Fig. 5), in agreement with the conclusions of Ref. 8. It is precisely in this region that the number  $N$  of vortices in the blocks changes, since the diffusion coefficient in the vortex system varies as  $TN/\eta$ . From the  $V_M(T)$  dependence in this region one can assess the value of  $N$  and the  $N(T)$  dependence; all that is necessary is to normalize the diffusion coefficient to the experimental data in the limit as  $N \rightarrow 1$ . We have neglected here the temperature dependences of the term in (9) connected with the pinning. As can be seen from Fig. 3, in some cases, and particularly in ours, this can be done because of the small variation of  $f_p$  and  $\eta$  in the considered temperature interval. On the presented experimental dependence (Fig. 5), the first point (corresponding to the highest temperature) differs with respect to  $V_M$  from the second by a factor of 3, and from the third by an order of magnitude and  $\partial V_M / \partial T|_{T=T_M} \gg \partial V_M / \partial T|_{T > T_M} \approx 0$  (the derivatives are considered at the extreme points of the curve of the inset in Fig. 5). Therefore, assuming (5) and (6) to be valid at  $T \approx T_M$ , we can assume with good accuracy (at least for all points starting with the second) that the presented  $V_M(T)$  dependence coincides with the function  $N(T)$ . If this dependence (inset of Fig. 5) is replotted in a log-log scale, it is found that a very good agreement with the experimental data is given by the functional relation  $N \propto (1 - T/T_c)^3 T$ . The experimental  $V_M(T)$

TABLE I.

| $d$    | $T_c, K$ | $T_M, K$<br>experiment | $T_M^0, K$<br>theory | $\Delta T, K$ | $\Delta T/T_M^0$    |
|--------|----------|------------------------|----------------------|---------------|---------------------|
| 1000 Å | 1,405    | 1,333                  | 1,394                | 0,061         | $4,4 \cdot 10^{-2}$ |
| 500 Å  | 1,43     | 1,268                  | 1,408                | 0,140         | $9,9 \cdot 10^{-2}$ |
| 300 Å  | 1,592    | 1,283                  | 1,550                | 0,267         | $17 \cdot 10^{-2}$  |

dependence normalized to the total number of vortices in the sample at  $T = T_M$  can be used to determine the number of vortices in the block and the variation of this number with temperature.<sup>3)</sup>

The number  $N$  of vortices in a block can be estimated also from the delay  $V$  of the secondary voltage [Eq. (9)]. At the point corresponding to the "critical current" of the secondary film we have  $\Delta V = f_p LH / c\eta N$ . For the temperature corresponding to curve 15 of Fig. 3 we have then  $N \sim 100$ . Thus, the Giaever-transformer method has made it possible not only to observe the phase transition in a system of two-dimensional vortices, but can also provide information on specific details of this process.

The author thanks N. Ya. Fogel' and L. I. Glazman for helpful discussions.

<sup>1)</sup>The method does not make it possible to come close enough to the critical point  $H_{c2}$  or  $T_c$ , especially in the case of thin films, where considerable overheating of the sample and an appreciable change in the induction of the magnetic field above it can occur when the ferromagnetic particles are pulverized.

<sup>2)</sup>Singularities of the impedances of thin films were observed in Refs. 5 and 6 at  $T > T_M$ . The authors emphasize there the difficulty of analyzing the

experimental situation and draw no decisive conclusion concerning the melting of the lattice.

<sup>3)</sup>If the films of the transformer are not identical, the lattice melting can take place initially in only one of them. The theory of Ref. 8 gives in this case the stronger dependence  $V_{2M}(T) \propto (1 - T/T_c)^3 [1 + T/T_c]^{-1}$ , which is comparable with the experimental data as  $T \rightarrow T_c$ . A strong argument against this explanation of the  $V_{2M}(T)$  dependence is the fact that shift predicted by the theory of Ref. 8 for the position of this maximum on the secondary IVC is not observed.

<sup>1)</sup>D. S. Fisher, Phys. Rev. **B22**, 1190 (1980).

<sup>2)</sup>R. P. Huebner, *Magnetic Flux Structures in Superconductors*, Springer, 1979.

<sup>3)</sup>A. I. Larkin and Yu. N. Ovchinnikov, J. Low Temp. Phys. **34**, 409 (1979).

<sup>4)</sup>J. M. Kosterlitz and D. J. Thouless, J. Phys. **C6**, 1181 (1973).

<sup>5)</sup>A. T. Fiory and A. F. Hebard, Phys. Rev. **B25**, 2073 (1982).

<sup>6)</sup>P. Martinoli, M. Nsabimana, G. A. Racine, H. Beek, and J. R. Clem, Helv. Phys. Acta **56**, 765 (1983).

<sup>7)</sup>G. Eilenberger and H. Buttner, Z. Phys. **224**, 335 (1969).

<sup>8)</sup>L. I. Glazman and N. Ya. Fogel', Fiz. Tverd. Tela (Leningrad) **26**, 800 (1984) [Sov. Phys. Solid State **26**, 482 (1984)].

<sup>9)</sup>J. W. Ekin, B. Serin, and J. R. Clem, Phys. Rev. **B9**, 912 (1974).

<sup>10)</sup>L. I. Glazman and N. Ya. Fogel', Fiz. Nizk. Temp. **9**, 210 (1983) [Sov. J. Low Temp. Phys. **9**, 104 (1983)].

<sup>11)</sup>M. A. Biondi and M. P. Garfunkel, Phys. Rev. **116**, 862 (1959).

Translated by J. G. Adashko